

Scattering Tomography Using Ellipsoidal Mirror

Ryuichi Akashi*, Hajime Nagahara*, Yasuhiro Mukaigawa† and Rin-ichiro Taniguchi*

*Kyushu University

744, Motooka, Nishi-ku, Fukuoka, 819-0395, Japan

†Nara Institute of Science and Technology

8916-5, Takayama, Ikoma, Nara, 630-0192, Japan

{akashi,nagahara,rin}@limu.ait.kyushu-u.ac.jp

mukaigawa@is.naist.jp

Abstract—Optical tomography provides visual images of the interior of objects. There are various methods depending on how the material behaves under scattering. If scattering is weak, one approach extracts the scattering amplitudes from the inputted projected images and estimates a cross-sectional image from images without scattering. Conversely, if the scattering is strong, an approach is to use the scattering amplitude to estimate the cross-sectional image. In this situation, light paths are scattered and a large field of view is required to observe all of the scattered light from which to construct the image. In this paper, we propose a method based on computed tomography which employs wrap-around viewing. We implement a projector-camera system that can send and then with an ellipsoidal mirror receive light scattered from an object from all fields of view. In addition, this system with mirror does not need any mechanical motion to capture scattered light during scanning.

I. INTRODUCTION

Visualizing the interior of an object is very useful and has already achieved some practical applications. For example, X-ray computed tomography (X-ray CT) is used in the medical field to provide clear cross-sectional images of specific areas of a human body using X-ray. Although X-rays have high transmissivity through human tissue enabling non-scattered projected images to be constructed, over-exposure to X-rays is a worrying medical issue. Diffuse optical tomography (DOT)[1] uses near-infrared light to obtain projected images and is safe for humans. However, the beam is easily scattered in the body and causes blurring in the projected images. Constructing clear cross-sectional images is difficult because of the blurring. To solve this problem, various methods have been proposed that remove the scattered light and recover shape projected images.

Treibitz et al. [2] proposed a descattering method using a polarizer and Nayar et al. [3] removed the scattered light by projecting a high-frequency pattern. However, these descattering methods can be applied only if scattering is weak because the component of transmitted light is very small if scattering is otherwise.

When scattering is strong, some methods model light scattering and use the scattering effect to estimate a cross-sectional image. Ishii et al. [4] proposed a Monte Carlo voting method, which estimates the distribution of obstacles in the scattering media. They simulate the light paths within the scattering media by Monte Carlo ray-tracing. The rays are various light

paths in the scattering media and exit the object at different locations before impinging the detector. They estimate the cross-sectional image by a voting process.

However, this method requires the detector to be placed on the opposing side of the light source. The field of view of the detector is then narrow and much of the scattered light falls out of the field of view and lost.

In this paper, we propose a method of scattering tomography which takes views a target object from all around the object. We also propose and prototype a projector-camera system with an ellipsoidal mirror. We can project the light and view the object from a full angular field of view using reflections from ellipsoidal mirror. The advantage of this setup is that we no longer need to mechanically rotate the light source and detector as in conventional CT scanners. We are able to speed up capturing times as well as obtain complete wrap-around viewing.

II. SIMULATING LIGHT PATH IN SCATTERING MEDIA

If the scattering is strong, it is necessary to simulate the light paths in the target object. We use Monte Carlo ray-tracing [5] for this purpose. In this model, the light paths are randomly generated. When light is scattered (Fig. 1), the propagation rate E is expressed as

$$E = \mu_s p(\cos \theta) \exp(-(\mu_s + \mu_a)(d_1 + d_2)), \quad (1)$$

where μ_s and μ_a are the scattering and absorption coefficients, respectively, which are defined as the probability of light scattering /absorption per unit infinitesimal path length. $p(\cos \theta)$ is the probability distribution for $\cos \theta$ and described by

$$p(\cos \theta) = \frac{1}{4\pi} \frac{1 - g^2}{(1 + g^2 - 2g \cos \theta)^{\frac{3}{2}}}, \quad (2)$$

where g is a parameter which describes the anisotropy of scattering and has a value between -1 and 1 . By using anisotropy g and random number ξ which is distributed between the interval $(0, 1)$, $\cos \theta$ is described by

$$\cos \theta = \begin{cases} 2\xi - 1 & (g = 0) \\ \frac{1}{2g} \left(1 + g^2 - \left(\frac{1-g^2}{1-g+2g\xi} \right) \right) & (otherwise). \end{cases}$$

To generate the light path, we iterate this calculation until the light path has exited the object or has been completely

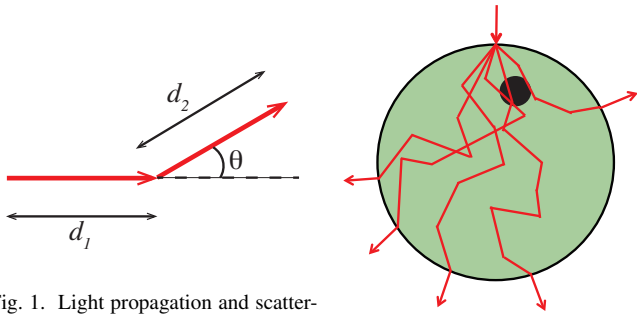


Fig. 1. Light propagation and scattering

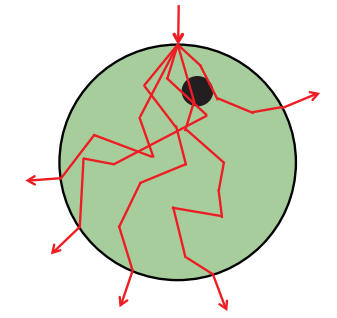


Fig. 2. Light paths in the presence of a single obstacle

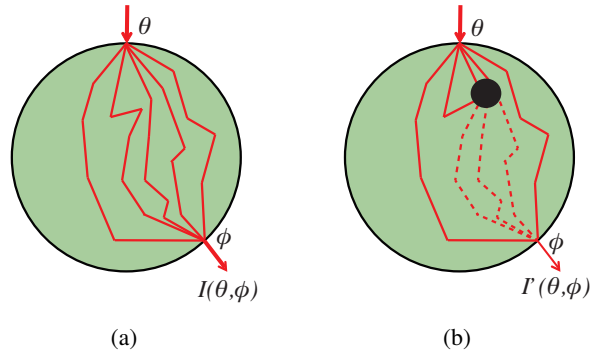


Fig. 3. Influence of obstacles on intensities: (a) light paths with no obstacles present; (b) the blocking of some of the light paths with an obstacle present; θ is incident angle of light, and ϕ is the emission angle.

absorbed by the object. After calculating an enormous number of light paths, we can simulate light scattering through objects with any number of obstacles Fig. 2.

III. ESTIMATING CROSS SECTIONAL IMAGE FROM WRAP-AROUND VIEWING

A. Problem Setting

Our objective is to estimate the distribution of obstacles in a scattering object. We assume that the scattering object is homogeneous and that there are no reflections from the surface of scattering object and each obstacle. We can then determine the scattering and absorption coefficients uniquely when the scattering object is known. The target object was taken to be a cylinder containing several obstacles. We captured the light ray intensities from all around the object employing wrap-around viewing.

B. Estimating Cross Sectional Image by Monte Carlo Voting

In this section, we explain the method of estimating the distribution of obstacles in a scattering object. To construct a cross-sectional image, it is necessary to irradiate the target object from various directions and to observe the light that passes through the object. Assuming no obstacles are present in the target object, we denote the observed intensity by $I(\theta, \phi)$, where θ is the light source direction and ϕ is the observing angle. Numerous light paths are associated with each pair of angles θ and ϕ [Fig. 3-(a)], and each path is calculated using Monte Carlo ray-tracing. Similarly, we define $I'(\theta, \phi)$ as the observed intensity in the presences of obstacles. In such circumstances, light paths can now be terminated on the surface of obstacles [Fig. 3-(b)]; their subsequent paths are represented as dashed lines to indicate that these paths have been blocked. Hence, with blocked paths and less light, $I'(\theta, \phi)$ is smaller than $I(\theta, \phi)$. We define the attenuation ratio $AR(\theta, \phi)$ as

$$AR(\theta, \phi) = \frac{I'(\theta, \phi)}{I(\theta, \phi)}, \quad (3)$$

and estimate the distribution of obstacles by choosing a value for $AR(\theta, \phi)$ for each light path entering with angle θ and exiting with angle ϕ because the intensity $I'(\theta, \phi)$ depends on the distribution of obstacles.

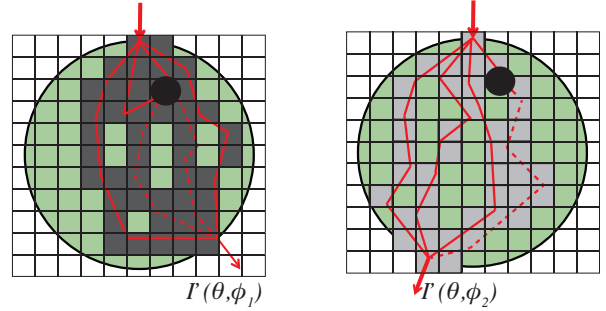


Fig. 4. Assigning process. (Left) With many blocked paths, a small value is assigned; (Right) With few blocked paths, a large value is assigned.

We explain the choice for exiting angles ϕ_1 and ϕ_2 (Fig. 4). If $I'(\theta, \phi_1)$ is much smaller than $I(\theta, \phi_1)$, the probability that obstacles exist on the light paths entering at angle θ and exiting at angle ϕ_1 , is high. We then assign a small value of $AR(\theta, \phi_1)$ to these paths (left image of Fig. 4). In contrast, if $I'(\theta, \phi_2)$ is similar to $I(\theta, \phi_2)$, we choose a large value which is close to 1 for the associated paths entering at angle θ and exiting at ϕ_2 (right image of Fig. 4). We iterate this assignment process for each pairing (θ, ϕ) . An area where there is an accumulation of small assignment values means that the probability of the presence of obstacles is high, because small values correspond to light paths on which obstacles are likely to be present.

C. Merit of Wrap-around Viewing

In regular computed tomography the configuration is such that the detector is placed on the opposite side to the light source; the detector observes a limited field of view. Ishii et al. [4] used this configuration in capturing projected images (Fig. 5) and estimating the cross-sectional image using Monte Carlo Voting. If we have a narrow field of view of the structure, we lose much information from lost rays, such as $L1$ and $L2$ in Fig. 5. These rays fall out of the field of view, because they are scattered in various direction from scattering media containing obstacles. In contrast, if we obtain full field-of-view observations using a wrap-around detector configuration (Fig. 6), we can observe all light paths as projected images. As

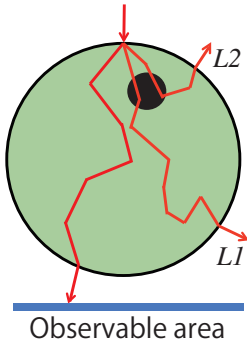


Fig. 5. Single angular viewing

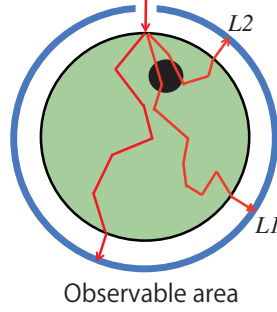


Fig. 6. Wrap-around viewing

a result, we can estimate more accurately the cross-sectional images using a similar Monte Carlo Voting.

Moreover, we can detect light from paths such as $L2$ which are near the light source (Fig. 5). These rays are only slightly affected by scattering because the path length of light is very short. Hence, it is very useful to determine whether an obstacle is present on such paths.

IV. SIMULATION EXPERIMENT

We estimated the distribution of obstacles in the scattering object using Monte Carlo Voting in a simulation experiment. We assumed a cylindrical object with either one or two obstacles and generated simulated projected images by ray-tracing. Figs. 7(a) and (b) show the configuration of the object with a single obstacle and the resulting image estimated from wrap-around viewing intensities. For comparison, Fig. 7(c) shows the resulting image estimated from a single directional view similar to Ishii's method for comparison. Fig. 8 shows images for the object with two obstacles. We can see that wrap-around viewing is more accurate than single-direction viewing (Figs. 7 and 8), confirming that wrap-around viewing has an advantage in estimating cross-sectional images.

V. IMPLEMENTATION

A. Wrap-around Viewing Using Ellipsoidal Mirror

To perform wrap-around viewing required in estimating the cross-sectional image, we propose a projector-camera system with an ellipsoidal mirror (Fig. 9). The ellipsoid has the property that light passing through one of its focal points is reflected toward the other focal point. Our proposed system with mirror (Fig. 10) uses a projector as a light source. The principal points of the camera and projector lenses correspond to one focal point of the ellipsoidal mirror, and the scattering object is placed at the other focal point. We arrange the camera and projector to be optically at the same focus point using a beam splitter. Fig. 11 shows the bench setup of our projector-camera system. Target object is set at center of ellipsoidal mirror. The camera and the projector are arranged optically same position toward the ellipsoidal mirror.

The emitted light from the projector is reflected onto the scattering object by the ellipsoidal mirror. The light that is

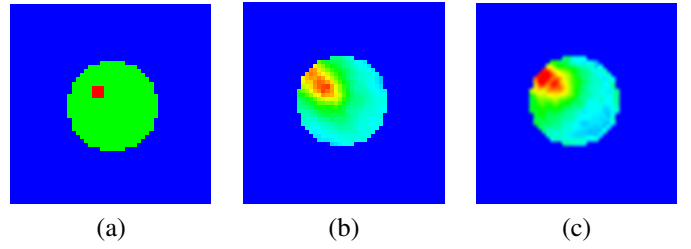


Fig. 7. Experimental results with a single obstacle. (Left) actual configuration with green indicating scattering media, red indicating an obstacle; (Middle) image from wrap-around viewing; (Right) image from single-direction viewing.

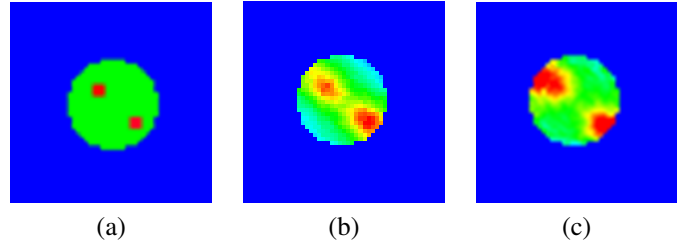


Fig. 8. Experimental results for an object with two obstacles. (Left) actual configuration; (Middle) image from wrap-around viewing; (Right) image from single-direction viewing.

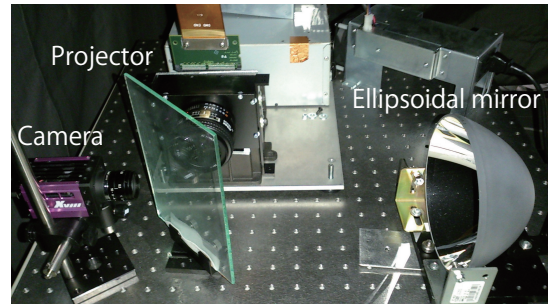


Fig. 11. Projector-camera system

scattered by and passes through the target object is reflected back and directed toward the camera lens at the other focal point. In consequence of this setup, we can observe scattering rays from all around the object. With the proposed system, we can easily change the light source direction by changing the display pattern of the projector. In contrast, the light source and detector in regular computed tomography are both mechanically rotated. Hence, needing no mechanical motion, our system can therefore speed up image capturing.

B. Camera-Projector Alignment

In our projector-camera system, the principal points of the camera and projector lenses have to be aligned with the focal point of the ellipsoidal mirror. Positional alignment of the camera and projector with respect to the ellipsoidal mirror is crucial. For this purpose, we used a method proposed by Amano et al. [6] employing a slit board (Fig. 12(a)). We assume that the camera and projector are already calibrated and their intrinsic parameters are known.



Fig. 9. Ellipsoidal mirror

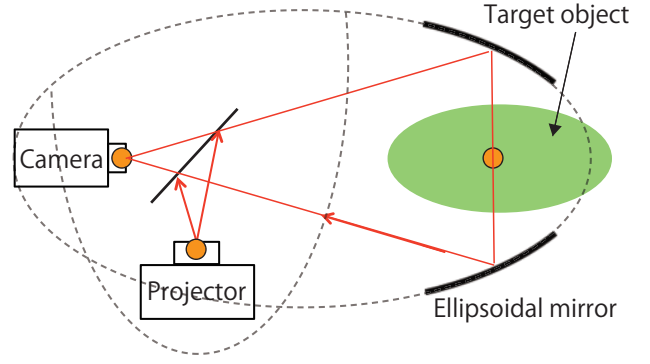


Fig. 10. Configuration of the optical system for wrap-around viewing

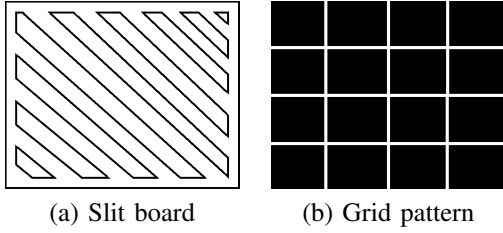


Fig. 12. (a) Slit board and (b) projected grid pattern.

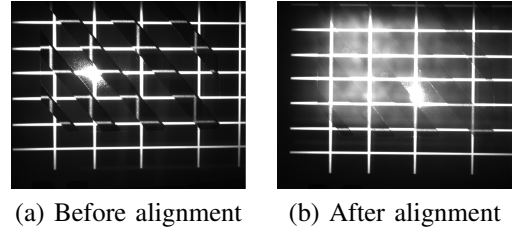


Fig. 14. Alignment result

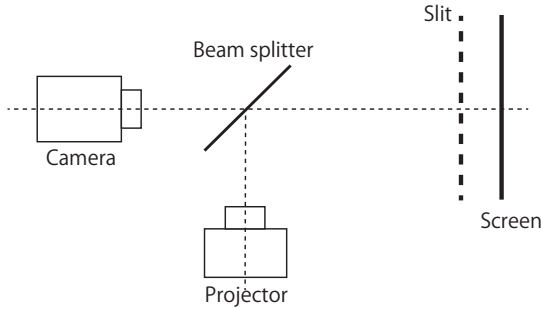


Fig. 13. Optical layout during alignment

During aligning, we replaced the ellipsoidal mirror with a screen and placed the slit board in front of the screen. Fig. 13 shows the optical layout during the camera-projector alignment. We then projected the grid pattern [Fig. 12(b)] from the projector toward the slit board and screen. With the initial camera position, we obtain an image similar to that shown in Fig. 14(a). The lines of the projected grid pattern are disconnected, and this discontinuity is caused by the misalignment of the camera and projector. By this misalignment visualization, we can manually adjust the camera position to produce smooth continuous grid lines [Fig. 14(b)].

VI. EXPERIMENTAL RESULTS FOR A REAL OBJECT

We now describe the estimation of the distribution of obstacles in a scattering media of a real object. We used the projector-camera system described in section V. For the scattering media, we used a target object made from silicon resin

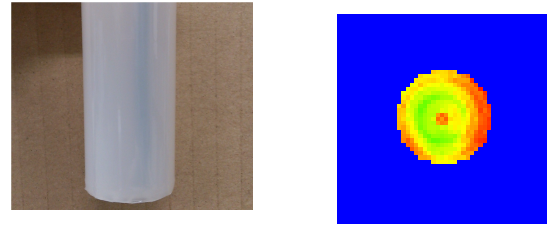


Fig. 15. Cylindrical scattering object made of silicon resin with a single metal obstacle.

Fig. 16. Image obtained using wrap-around viewing.

and metal wires as obstacles. The target object is cylindrical in shape with diameter of 27 mm (Fig. 15). The wire is seen as the darkened filament inside object.

We give an image for the estimation of the obstacle distribution for this real object (Fig. 16). Red areas signify a higher probability of an obstacle being present within the area. From the result of the estimation, the central and peripheral areas of the object indicate high probability of a presence, in particular, on the side where the metal wire actually is. However, the result of the estimation in this experiment is not accurate. We believe that the estimation error is caused by the specular reflection from the object's surface. In calculating the light paths in the object by Monte Carlo ray-tracing, we eliminated all reflections of incident light from obstacles. Thus, paths were being blocked by obstacles both in transmission and reflection and hence reduced the intensities further.

VII. CONCLUSION

We proposed a tomography method using wrap-around viewing, and implemented a projector-camera system. Our

projector-camera system can illuminate and view an object with full 360°-angular views without requiring mechanical motion. In a simulation experiment, we demonstrated that a more accurate distribution of obstacles is obtained by wrap-around viewing than by single-direction viewing. We experimented with a real object, but could not obtain an accurate estimate because reflections from the obstacle's surface were omitted in Monte Carlo ray-tracing.

For the future, we will be removing the effects of specular reflections of incident light to improve image estimations. Additionally, we will be considering means to perform multiple lighting at various angular views simultaneously to try to shorten image capturing times.

REFERENCES

- [1] D. A. Boas, D. H. Brooks, E. L. Miller, C. A. DiMarzio, M. Kilmer, R. J. Gaudette, and Q. Zhang. "Imaging the body with diffuse optical tomography." *IEEE Signal Processing Magazine*, 18(6):55-75, 2001.
- [2] T. Treibitz and Y. Y. Schechner. "Active polarization descattering." *Pattern Analysis and Machine Intelligence, IEEE Transactions on* 31.3 (2009): 385-399.
- [3] S. K. Nayar, G. Krishnan, M. D. Grossberg, and R. Raskar. "Fast separation of direct and global components of a scene using high frequency illumination." *ACM Transactions on Graphics*. Vol. 25. No. 3. ACM, 2006.
- [4] Y. Ishii, T. Arai, Y. Mukaigawa, J. Tagawa, and Y. Yagi. "Scattering tomography by Monte Carlo voting." *International Conference on Machine Vision Applications*. 2013.
- [5] L. Wang, S. L. Jacques, and L. Zheng. "Mcml-Monte Carlo modeling of light transport in multi-layerd tissues." In *Computer Methods and Programs in Biomedicine* 47, pages 131-146. Elsevier, 1995.
- [6] T. Amano. "Projection Center Calibration for a Co-located Projector Camera System." *Computer Vision and Pattern Recognition Workshops, IEEE*, 2014.